CFD and Experimental Study in the Optimization of an Energy Converter for Low Heads

Ramos, H. M.[a],*; Simão, M.[b]; Borga, A.[b]

[a] Professor of Instituto Superior Tecnico (IST), Civil Engineering Department (DECivil) – CEHIDRO researcher, Lisbon, Portugal.
[b] MSc degree of Instituto Superior Tecnico (IST), Civil Engineering Department (DECivil) – CEHIDRO researcher, Lisbon, Portugal.
*Corresponding author.

Abstract

This paper deals with new design of low head turbines, as feasible solutions to solve the lack of energy in rural and remote areas, or to provide energy from urban water pipe systems. Propeller turbines are then the subject of this research because they are suitable for small heads, discharges with little variability, easy to manufacture and with low costs associated. Hence, the aims are the design of quite simple tubular propeller turbines and the analysis of hydrodynamic behaviour for different number and configuration of blades, based on CFD analyses and experimental tests development. An advanced hydrodynamic code based on the finite volume method, as well as blades configuration and mesh specific models are used for the impeller and the turbine design. The blade geometry is optimized using mathematical formulations and experimental results, concerning the possible range of operation under best efficiency conditions. Performance curves are obtained for typical characteristic parameters allowing comparisons between CFD and experimental results. Based on the similarity theory applied to turbomachines it is possible to evaluate the hydrodynamic behaviour through a tubular propeller for different sizes, in a scale model application.

Key words: Low head turbines; Fluid dynamics; Tubular propeller; CDF analysis; Performance curves

INTRODUCTION

Hydrodynamic models of fluid mechanics, also known by computational fluid dynamics (CFD), allow the evaluation of the flow behaviour, for a specific system configuration with associated boundary conditions. These models need the development of theoretical analysis on the physical behaviour of the flow based on mathematical formulations in three-dimensional analyses, with enough accuracy not only for laminar and turbulent flows, but also for the various forms of energy transfer, changing phases of the flow, vorticity occurrence, levels of turbulence and shear stress between interfaces. Hence, this study deals with a new propeller solution based on a facility implementation in order to predict the real evaluation of the pathlines, turbulence and losses effects, for different operating conditions.

Pico turbines are cost effective means of producing electricity of low power being under analysis for new improvements, despite the less attention that researchers and manufactures have been paid to those engines' technology. Thus, the challenge of this work is therefore to provide new engineering designs and implementation methods that can be effectively customized and applied for possible energy recovery projects in water systems of low head and relative flow rates, such as from natural small rivers or streams, water supply, irrigation and drainage systems, treatment plants or aquaculture factories.

Definitions for pico-hydropower vary, but the term generally refers to power systems below 5 kW. At isolated regions, such systems are suitable for individual households and powering data loggers or management control systems in water companies.

A fixed geometry propeller turbine was built and tested for a runner speed of 1000 rpm, suited to 35 m head and about 5 l/s flow rate, reaching good efficiencies (Howey, 2009). It was also designed and installed in field a fixed geometry propeller turbine with a spiral casing showing an overall mechanical efficiency of 65%

(Simpson & Williams, 2006). Recent optimizations of low-head axial-flow hydro turbines have enabled to reach interesting operating efficiencies. Several researchers (e.g. Demetriades, 1997; Upadhyay, 2004; Alexander *et al*., 2009) have developed models of medium sizes for propellers turbines, but until now there are no any relevant expression studies for propellers working as micro turbines, allowing new developments of improvements in its design, efficiency and versatility of operation based on both computational modelling and experimental analysis. A new fixed blade runner called "mixer" suitable for upgrading old units of Francis turbines installed in low head hydropower plants was recently developed by (Skotak, 2009). This new turbine suitable for a head of 5 m, with a runner diameter of 2250 mm and a discharge of 23 m^3/s allows obtaining higher efficiency by optimizing the shape of the runner blades.

These new design solutions are usually appropriate to hydropower schemes with large discharge values, leaving an open field for developing new geometries optimization models with smaller sizes, in order to cover a large range of applications, where low power are available, especially in water pipe systems.

Through turbo machine similarity it is possible to estimate different operating conditions from an equivalent turbine, even though the scale effects associated. The behaviour of the system as a whole can differ, depending on the scale adopted, and the configuration of the runner, in particular the blades shape (Ramos *et al*., 2009). Consequently, the design and the development of micro turbines cannot be only based on the methodology of exactly scaling down from large turbines. Economic, hydrodynamic and manufacturing constraints give opportunities to create new designs adequate to each type of water system or infrastructure, depending on its main characteristics.

This study provides analysis based on a new blade model configuration and CFD analysis, as well as new hydraulic energy converters suitable for applications of micro-scale for low head and flow rate conditions, which can be easily implemented both in remote areas, as well as in water pipe systems in urban environment, with non-negligible flow energy available that would be wasted or dissipated. The proposed new tubular propeller turbines (with 4 and 5 blades) represent a cheap and easy installation solution to cover a range of low power, head and discharge values which are not available in the market.

1. FLUID DYNAMICS

1.1 Fundamentals

In computational fluid dynamics, the CFDs are important tools to estimate real results from the calibration based on experimental tests, which allow for better understanding the phenomenon associated with the flow behaviour in turbines for different flow conditions (Ramos *et al*., 2010). In fact, these CFD are advanced models of fluid mechanics widely used in the analysis of complex in setting hydraulic systems, leading to optimal design solutions. FLUENT is a hydrodynamic model that applies the technique of finite volumes to solve the equations that describe the flow, as the continuity equation and the Euler or Navier-Stokes' equations also known as Reynolds equations. This model features two types of calculation algorithms that can be solved by a system of equations. Regarding the latter option the algorithm SIMPLE is a way to resolve the coupling between velocity and pressure. In the case of Reynolds stress it is used the k-ε model since it is a robust model with proven results on the turbulence analyses. The model includes two equations regarding the properties of turbulence flow, which allows accounting for all purposes of the convection and diffusion of the turbulence intensity. One of the variables is the turbulent kinetic energy, k, while the other represents the rate of dissipation, ε. In summary the dissipation variable determines the scale of turbulence, while the kinetic energy the turbulence intensity.

1.2 k-ε Model

The effect of turbulence normally occurs for high values of Reynolds, and is the cause of production some eddies within the fluid. Associated with turbulent flow it can be identified zones with rotation, diffusion intermittence, highly disordered and dissipative effects. Regions with greater turbulence, which are normally associated to fluctuations of low frequency, can be considered as a boundary condition of the flow and its size can reach the same order of magnitude of the flow itself. As a result, turbulent flow characteristics require specific models to determine the correlation between velocity and pressure. According to the simplifications in the fluid transport equation (Equation (1)), it is possible to make a parallel between these equations and those used by the turbulence k-ε model.

$$\rho \frac{\partial u_j}{\partial t} + \rho u_i \frac{\partial u_j}{\partial x_i} = \rho g_i - \frac{\partial p}{\partial x_j} + \frac{\partial}{\partial x_j}\left(\lambda \frac{\partial u_i}{\partial x_i}\right) +$$

$$\frac{\partial}{\partial x_i}\left[\mu\left(\frac{\partial u_i}{\partial x_j} + \frac{\partial u_j}{\partial x_i}\right)\right] \tag{1}$$

This k-ε model is a semi-empirical based on transport equations of kinetic energy turbulent (k) and its dissipation rate (ε). The flow transport equations for the k model, are derived from the exact equation, while the transport equation for the ε model is obtained through physical relations (Fluent, 2006). In the derivation of the k-ε model it is assumed the flow is turbulent, and the effects of molecular viscosity are negligible. Thus, the turbulent kinetic energy and its dissipation rate are obtained, respectively, by Equations (2) and (3):

$$\frac{\partial(\rho k)}{\partial t} + \frac{\partial(\rho k u_i)}{\partial x_i} = \frac{\partial}{\partial x_j}\left[\left(\mu + \frac{u_t}{\sigma_k}\right)\frac{\partial k}{\partial x_j}\right] + P_k - \rho\varepsilon \qquad (2)$$

$$\frac{\partial(\rho\varepsilon)}{\partial t} + \frac{\partial(\rho\varepsilon u_i)}{\partial x_i} = \frac{\partial}{\partial x_j}\left[\left(\mu + \frac{u_t}{\sigma_k}\right)\frac{\partial\varepsilon}{\partial x_j}\right] + \frac{\varepsilon}{k}\left(C_{1\varepsilon}P_k - C_{2\varepsilon}P_\varepsilon\right)$$

$$(3)$$

Where $C_{1\varepsilon}$, $C_{2\varepsilon}$ are constants, and σ_k, σ_ε correspond to the variables turbulent Prandtl k and ε, respectively, determined experimentally with air and water affected by friction in flows with homogeneous and isotropic turbulence (Scott-Pomerantz, 2004). The experience shows that these values provide good results for a wide range of defined border and free of friction. Once, the following constants were adopted: $C_{1\varepsilon} = 1.44$, $C_{2\varepsilon} = 1.92$, $\sigma_k = 1.0$, $\sigma_\varepsilon = 1.3$. P_k is the product of turbulence due to viscous forces and fluctuations,

$$P_k = \mu_t \nabla u\left(\nabla u + \nabla u^T\right) - \frac{2}{3}\left(\nabla u\right)\left(3\mu\nabla u + \rho k\right) + P_{kb} \qquad (4)$$

The turbulent dynamic viscosity, μ_t, is calculated by combining k and ε as follows:

$$\mu_t = \rho C_\mu \frac{k^2}{\varepsilon} \qquad (5)$$

Where, μ_t is defined as the turbulent dynamic viscosity and C_μ is an empirical constant specified in the turbulence model (approximately 0.09).

For high Reynolds numbers, the rate of kinetic energy dissipation is obtained by multiplying the viscosity with the fluctuating vorticity. An exact equation for the transport of vorticity floating is the rate of dissipation, which can be derived from the Navier-Stokes equations transforming the turbulent kinetic energy and the dissipation rate in Equations (6) and (7).

$$\frac{\partial k}{\partial t} + div(\rho u k) = div\left[\left(\mu + \frac{\rho v_t}{\sigma_k}\right)grad k\right] + \rho v_t G - \rho\varepsilon \qquad (6)$$

$$\frac{\partial\varepsilon}{\partial t} + div(\rho u\varepsilon) = div\left[\left(\mu + \frac{\rho v_t}{\sigma_\varepsilon}\right)grad\varepsilon\right] + C_{1\varepsilon}\rho v_t G\frac{\varepsilon}{k} - C_{2\varepsilon}\rho\frac{\varepsilon^2}{k} \qquad (7)$$

Where G and v_t are given by

$$G = 2\left(\left[\frac{\partial u}{\partial x}\right]^2 + \left[\frac{\partial u}{\partial y}\right]^2 + \left[\frac{\partial u}{\partial z}\right]^2\right) + \left(\frac{\partial u}{\partial y} + \frac{\partial v}{\partial x}\right)^2 + \left(\frac{\partial u}{\partial z} + \frac{\partial w}{\partial x}\right)^2 +$$

$$\left(\frac{\partial w}{\partial y} + \frac{\partial v}{\partial z}\right)^2 \qquad (8)$$

$$v_t = \frac{\mu_t}{\rho} \qquad (9)$$

To establish a first image of the turbulent regime, it is consider that the flow rate increases and the impeller rotational speed also rises induced by the gradient along the solid walls and the amounts up the viscous stresses.

However, the occurrence of different viscous tensions from point to point, determines the curved trajectories of the flow particles, a phenomenon which increases as they approach to the solid boundaries, given the increased role of concentrated stress gradients.

1.3 Mesh Specification

The success of 3D computational modelling in fluid mechanics requires a special attention during the mesh generation. When a flow passes through a turbine, the turbulence (from the effective viscosity variable in space) plays an important role in the dynamic convection, requiring that in complex flows, the amount of turbulence are duly solved with high precision. Due to the strong interaction between flow and turbulence, numerical results tend to be more susceptible to the grid dependency than for a laminar flow. Thus, it is recommended that the study considers sufficiently thin meshes in regions where occur rapid flow changes and concentrated large tangential tensions. In this way, the use of a mesh generation model (workbench-mesh creation) to describe the volumes, allows the calculation space and the appropriate definition of the boundary conditions (Ansys CFX, 2006).

For the mesh occupied by the flow, it is defined a physical preference in the CFD model and an initial control method, setting mesh defaults changing only one parameter "growth rate" to 1.5 since this value is crucial in the choice of the mesh size, concerning the number of elements and nodes. This model use an advanced size function where all the faces are identified, since the entire turbine, until the ones that correspond to more restrictions in places where the mesh is difficult to create, which usually coincides with rather small volumes. Thus, the mesh created on all sides surrounding the body of the impeller, comprised of the blades, interior bulb, and the shaft to connect the generator, corresponds to 333793 elements and 65103 nodes (Figure 1).
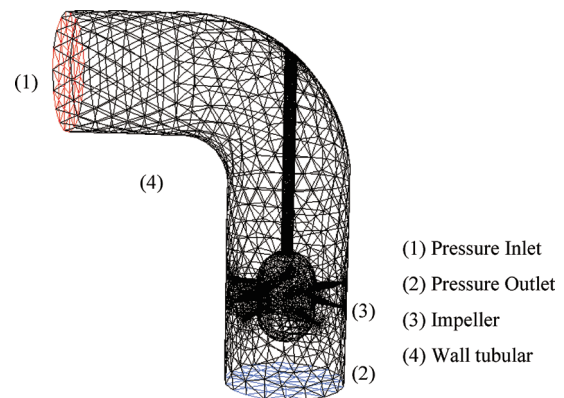

(1) Pressure Inlet
(2) Pressure Outlet
(3) Impeller
(4) Wall tubular

Figure 1
Schematic of the Mesh Created for a Tubular Propeller

The boundary conditions specify the values of characteristic variables in the physical limits of the device. As part of the simulations for each case study, there are four types of boundary conditions: inlet and outlet

pressure, rotor or impeller and the tubular wall. Areas designated by impeller are defined as moveable walls, with rotational speed around the rotation shaft, which corresponds to the centre of the runner. In other areas of the field corresponding to solid surfaces is imposed the condition of impermeability and uses the standard wall law for turbulent flow simulations. The faces of the elements belonging to periodic surfaces (the area occupied by the fluid) are treated as inner faces of the domain. All simulations were carried out with the fluid corresponding to water density and constant viscosity, with values of ρ = 998.2 kg/m^3 and n = 1.01×10^{-6} m^2/s.

2. BLADE MODEL CONFIGURATION (BMC)

In the design of the impeller blades it is important to analyse different slopes (i.e. angle variation) in order to determine the best results that lead to a best efficiency point (BEP). In the blades design it was adopted a minimal thickness as possible in order to avoid disturbances in the flow, causing additional losses that might constrain its effectiveness. For the flow rates considered in micro turbines, the maximum thickness of 1mm was taken into account for the blades due to limitations of the mesh generation. Figure 2 shows the velocities triangles to take in the optimization of the blade configuration. It shows the parameters are associated to each other from the direction of the blades, as the angle variation by the vectors indicated. Hence, a blade model configuration (BMC) was developed to estimate the best blade orientation to get the best efficiency operating conditions. It is a lengthy process that requires special care and sensitivity analyses to various characteristic parameters associated to the inlet and outlet velocity triangles.
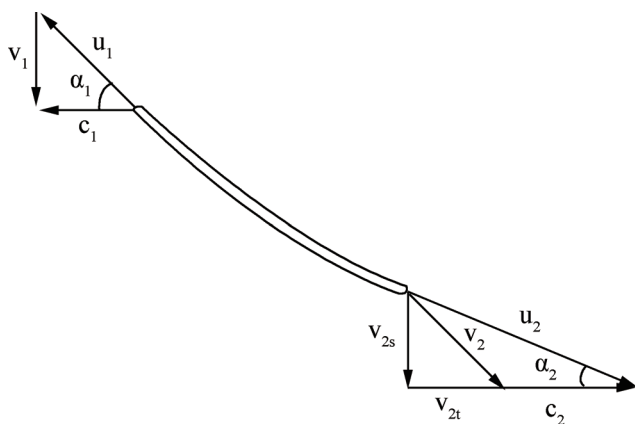

Figure 2
Velocity Vectors in a Blade of a Turbine Propeller

In Figure 2, velocity vectors are identified by the vectors of absolute (v), periphery (c) and relative runner blade velocity (u). From them and according to the shown detail in Figure 2, it is established some essential relationships to calculate the turbine discharge for a given configuration. Knowing the periphery velocity (c) at the inlet and outlet of a blade, which depends on the impeller rotational speed (ω) and the blade radius (r),

$$c_1 = c_2 = \omega\, r \qquad (10)$$

and the absolute velocity (v) depends on the discharge (Q) that pass through the impeller (Ramos *et al*., 2009),

$$v_1 = v_{2s} = \frac{Q}{S} = \frac{Q}{\pi\left(r_e^2 - r_i^2\right)} \qquad (11)$$

being S the tubular cross section area, r_e and r_i the tip and hub blade radius between the runner periphery and internal bulb, respectively.

According to the angles of a blade on the periphery of the inlet and outlet (subscript 1 and 2, respectively) of the impeller yields the following Equations (12) and (13),

$$tg\alpha_1 = \frac{v_1}{c_1} = \frac{Q}{S} \cdot \frac{1}{\omega\, r} \qquad (12)$$

$$tg\alpha_2 = \frac{v_{2s}}{c_2 + v_{2t}} = \frac{v_1}{\omega\, r + v_{2t}} \Leftrightarrow tg\alpha_2 = \frac{Q}{S}\left(\frac{1}{\omega\, r + v_{2t}}\right) \qquad (13)$$

To reduce the losses in the turbine, it is assumed the flow at downstream of the impeller is irrotacional, influenced by a vortex formation, depending on the radius of the blade, the flow cross-section and the discharge value as presented in Equation (14),

$$v_{2t} = \frac{k}{r} \Rightarrow k = -\omega\, r^2 + \frac{Q\, r}{S\, tg\alpha_2} \qquad (14)$$

In fact as the angle of the blade changes from the inlet to the outlet, between the upstream section, where the flow impulse the blade, to downstream section, the efficiency changes and may lead to better or worse values depending on the angle variation along the blade profile.

Based on the Equations (12) to (14), the blade model configuration determines the angles for a given rotational speed, leading to an optimum performance. The input values known as the head, discharge, rotational speed for the rated conditions, runner diameter, relation between the runner bulb and periphery diameter, the open blade angle (a$_p$) which depends on the number of blades, the angles of the inlet and outlet from the axis to the periphery in each blade are calculated, as well as the power, the specific speed and the constant vortex velocity by Equation (14). Knowing all the data provided by the input conditions, the correct blade configuration from the bulb section (r$_i$) to the periphery (r$_e$) (Figure 3) is then determined.
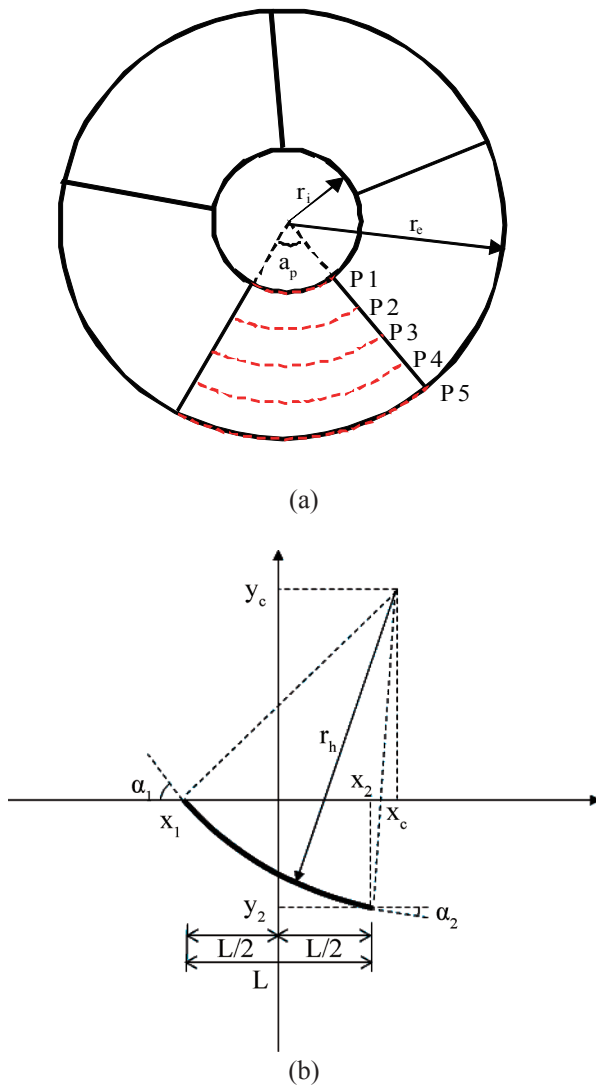
coordinates of the blade represented in Figure 3 (b); and r_h the radius of the blade curvature.

$$y_i = y_c - \sqrt{r_h^2 - (x_i - x_c)^2} \qquad (15)$$

$$x_i = x_2 + n_i \frac{x_1 - x_2}{n_j} \qquad (16)$$

The representation of the profiles on each blade configuration (Figure 3 (a)) corresponds to each line between (r_i) and (r_e), the bulb radius and the runner periphery, respectively.

As the upstream of momentum per unit time is given by Equation (17),

$$m = \rho Q v \qquad (17)$$

deriving it, the Equation (18) is then obtained,

$$dM_{2t} = \rho \ dQ \ v_{2t} = \rho \ v_1 2\pi r \frac{k}{r} dr \qquad (18)$$

which by algebraic manipulation yields Equation (19),

$$dM = dM_{2t} r = 2\rho \ k \ v_1 \pi r \ dr \qquad (19)$$

After its integration the binary is obtained by Equation (20),

$$M = \int_{r_1}^{r_2} dM = \int_{r_1}^{r_2} 2\rho \ k \ v_1 \pi r \ dr = 2\rho \ k \ v_1 \pi \int_{r_1}^{r_2} r dr =$$

$$2\rho \ k \ \pi v_1 \left(\frac{r_2^2}{2} - \frac{r_1^2}{2} \right) = \rho \ kQ \qquad (20)$$

As the motor or mechanical power is given by Equation (21),

$$P_{mec} = M\omega = \rho \ Q \ k \ \omega \qquad (21)$$

and the hydraulic power by Equation (22),

$$P_h = \gamma \ Q \ H \qquad (22)$$

the efficiency is given by Equation (23),

$$\eta_t = \frac{P_{mec}}{P_h} = \frac{\rho \ Q \ k \ \omega}{\gamma \ Q \ H} = \frac{k \ \omega}{gH} \qquad (23)$$

In order to design the tubular propeller to the available lab conditions, it is considered the outer impeller diameter of 100 mm, with a bulb diameter of 50 mm. According to Table 1 the blades design is built to operate with a discharge of 4 l/s at 300 rpm for the rotational speed.


(a)

(b)

Figure 3
Scheme of a Propeller: (a) Plan View with Five Blades and Five Profiles in a Blade; (b) Parameters Associated to the Tracing Profiles in Each Blade

The five profiles (i.e. P1 to P5) in each blade are then drawn from two fundamental equations (Equations (15) and (16)), where, j, represents the number of chosen points required to perform the tracing blade profile; y_c and x_c are the centre of the blade; x_1 and x_2 the inlet and outlet

Table 1
Values for the Blade Profiles Design

					5 blades					
	r(m)	tg(α_1)	tg(α_2)	α_1 (°)	α_2 (°)	L (m)	r_h (m)	x_1(m)	x_2(m)	x_c(m)	y_c(m)
P1	0.025	0.8646	0.2975	40.8	16.6	0.029	0.080	0.015	-0.015	-0.037	0.060
	0.028	0.7685	0.3066	37.5	17.0	0.033	0.105	0.017	-0.017	-0.047	0.083
P2	0.031	0.6917	0.3116	34.7	17.3	0.037	0.135	0.018	-0.018	-0.059	0.111
	0.034	0.6288	0.3131	32.2	17.4	0.040	0.173	0.020	-0.020	-0.072	0.146
P3	0.038	0.5764	0.3120	30.0	17.3	0.044	0.219	0.022	-0.022	-0.087	0.190
	0.041	0.5321	0.3090	28.0	17.2	0.048	0.274	0.024	-0.024	-0.105	0.242

To be continued

Continued

	r(m)	tg(α_1)	tg(α_2)	α_1 (^{0})	α_2 (^{0})	L (m)	r_h (m)	x_1(m)	x_2(m)	x_c(m)	y_c(m)
					5 blades						
P4	0.044	0.4941	0.3045	26.3	16.9	0.051	0.339	0.026	-0.026	-0.125	0.304
	0.047	0.4611	0.2990	24.8	16.6	0.055	0.417	0.028	-0.028	-0.147	0.378
P5	0.050	0.4323	0.2928	23.4	16.3	0.059	0.507	0.029	-0.029	-0.172	0.466
					4 blades						
P1	0.025	0.8646	0.2975	40.8	16.6	0.035	0.096	0.018	-0.018	-0.045	0.072
	0.028	0.7685	0.3066	37.5	17.0	0.040	0.126	0.020	-0.020	-0.057	0.100
P2	0.031	0.6917	0.3116	34.7	17.3	0.044	0.163	0.022	-0.022	-0.071	0.134
	0.034	0.6288	0.3131	32.2	17.4	0.049	0.208	0.024	-0.024	-0.087	0.176
P3	0.038	0.5764	0.3120	30.0	17.3	0.053	0.263	0.027	-0.027	-0.105	0.228
	0.041	0.5321	0.3090	28.0	17.2	0.057	0.329	0.029	-0.029	-0.126	0.291
P4	0.044	0.4941	0.3045	26.3	16.9	0.062	0.408	0.031	-0.031	-0.150	0.366
	0.047	0.4611	0.2990	24.8	16.6	0.066	0.501	0.033	-0.033	-0.177	0.455
P5	0.050	0.4323	0.2928	23.4	16.3	0.071	0.610	0.035	-0.035	-0.207	0.560
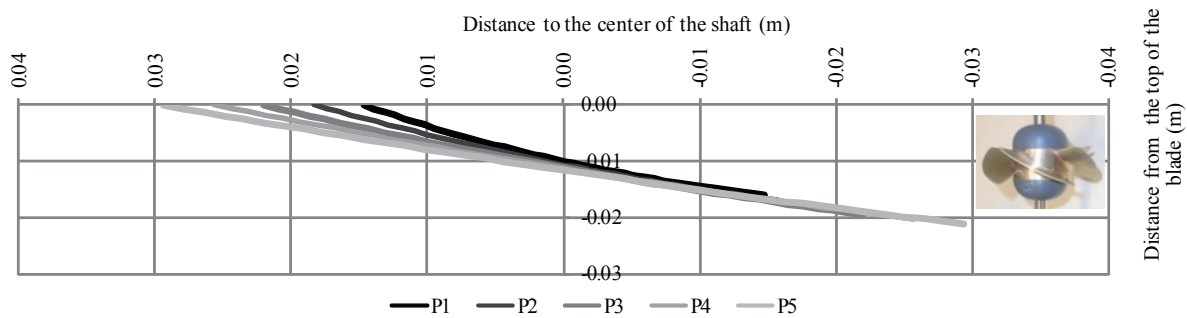
(a) Propeller with Five Blades
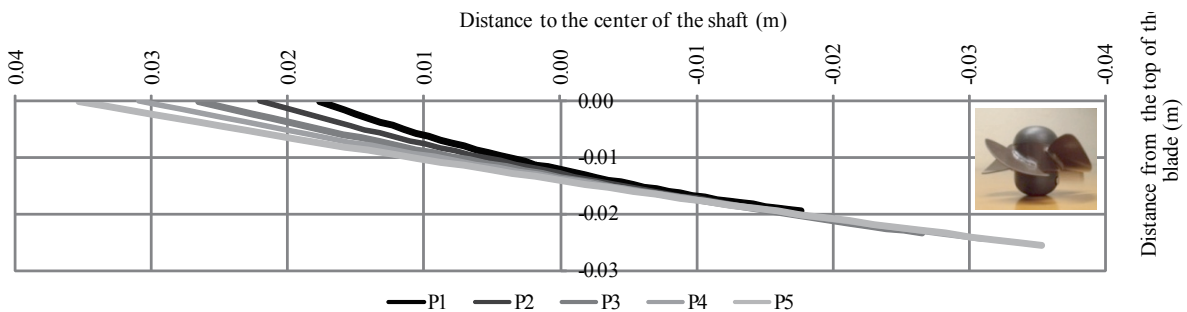
(b) Propeller with Four Blades

Figure 4
Design of Different Profiles for Each Blade (Impellers Configuration)

To design the blades profile presented in Figure 4 (for five (a) and four (b) blades) the variables presented in Table 1 are used in Equations (15) and (16).

3. CFD ANALYSES

3.1 Performance Curves

For the two designed impellers (with five and four blades)

which are characterised by its specific speed N_{sqt} as stated in Equation (24):

$$N_{sqt} = N \frac{\sqrt{Q}}{H^{0.75}} \qquad (24)$$

were developed comparisons between the blade model configuration (BMC) and CFD analyses. Table 2 confirms a good agreement between BMC (for a maximum

theoretical efficiency of 100 %) and the CFD simulations, even the existing losses, turbulence effects, anisotropy in zones of high flow circulation, scale effects, which are not considered in the theoretical methodology of the BMC. CFD simulations use, in a first stage, the angles obtained by BMC, but sensitivity investigation regarding the best efficiency operating conditions induces small corrections to those angles as shown in Table 2.

Table 2
Comparison Between Tip and Hub Angles for the Tubular Propeller with Five Blades

Characteristic parameters	Methodology			
	BMC		CFD	
	D = 100 mm	D = 200mm	D = 100 mm	D = 200mm
	N_{sqt} = 80 rpm		N_{sqt} = 77 rpm	
Inlet hub angle ($\alpha 1$) ($^{\circ}$)	41	46	44	
Outlet hub ange ($\alpha 2$) ($^{\circ}$)	17	11	21	
Inlet tip angle ($\alpha 1$) ($^{\circ}$)	23	24	26	
Outlet tip ange ($\alpha 2$) ($^{\circ}$)	16	14	19	
Power (W)	104	9967	104	9869

It is notorious the difference in power values of power between impellers diameter of 100 and 200 mm. This difference allows concluding that for the propeller with five-blades higher discharge values are need.

Two geometrically similar turbines operating at rotational speeds that satisfy the condition presented in Equation (25), have usually different values of efficiency in particular when the relationship between homologous lengths is high.

$$\frac{N}{N^{'}} = \left(\frac{H}{H^{'}}\right)^{1/2} \frac{D^{'}}{D} \qquad (25)$$

This is due to scale effects noticed between the two machines, driven by the effect of viscosity which causes loss of pressure, preventing thus a quadratic variation to the flow velocity. For different rotational speed values and flow conditions, the efficiency are obtained (Figure 5), for the tubular propellers with five and four blades.
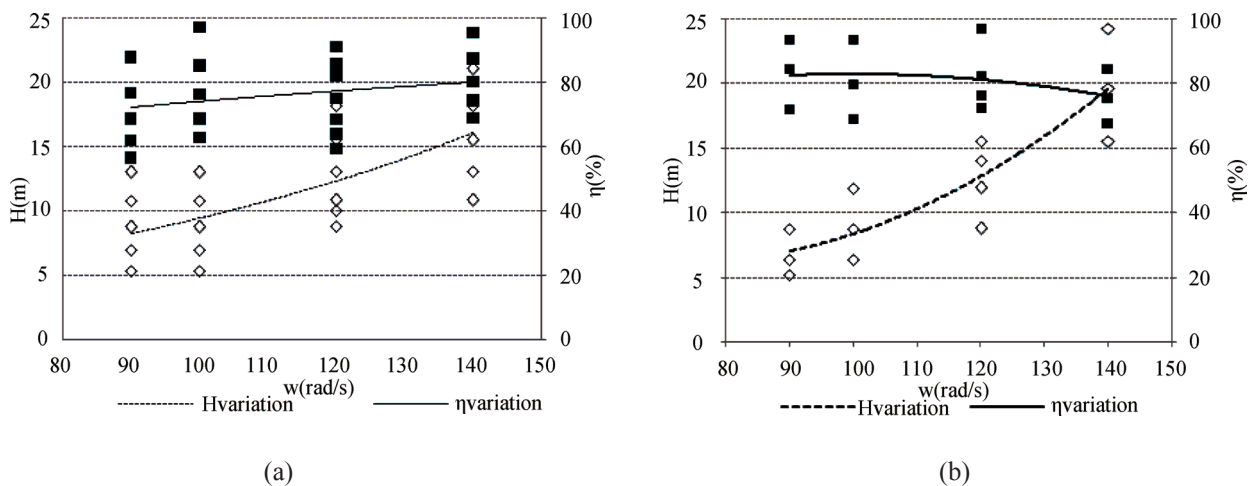

(a)

(b)

Figure 5
Performance Curves of Efficiency and Head Versus Rotational Speed, for a Runner Diameter of 200 mm: (a) with Four Blades; (b) with Five Blades
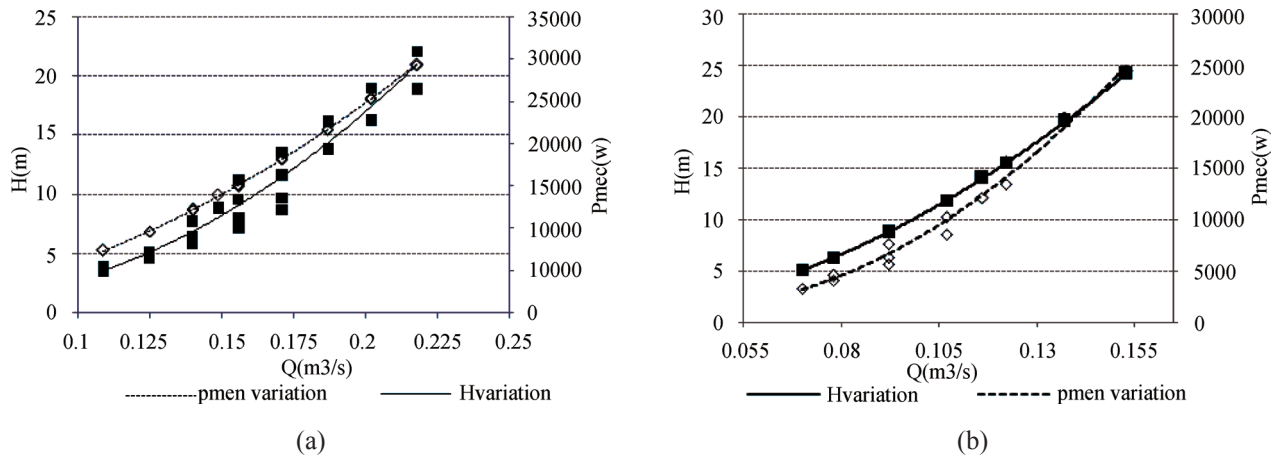
Figure 6
Performance Curves of Head and Mechanical Power Versus Discharge for a Runner Diameter of 200 mm: (a) with Four Blades; (b) with Five Blades
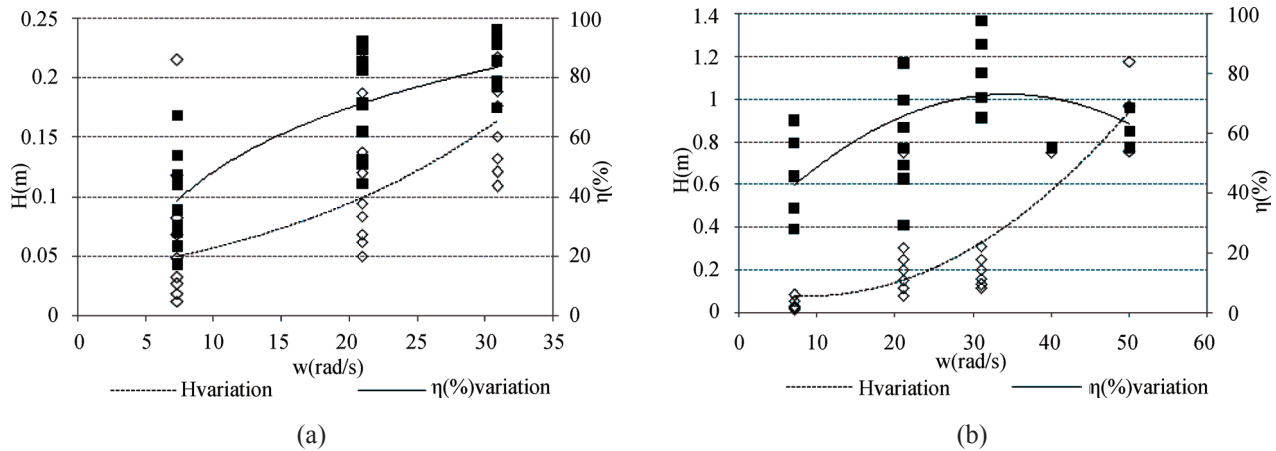

Figure 7
Performance Curves of Efficiency and Head Versus Rotational Speed, for a Tubular Propeller, with a Diameter of 100 mm: (a) with Four Blades; (b) with Five Blades

Figure 6 shows the curves of head and mechanical power versus discharge for the two impellers analyzed. In Figure 7, the turbine with a smaller runner diameter (D =100 mm) is performed and it is most suitable for small discharge values as happen with small drinking systems as well as in water distribution lab conditions in which the maximum discharge value is around 5 l/s.

Table 3
Reference Values for Tubular Propeller (D = 200 mm)

5 blades (200 mm)							4 blades (200 mm)					
Q_{ef} (m³/s)	M (N•m)	w (rad/s)	P_{mec} (W)	h (m)	P_h (W)	η (%)	Q_{ef} (m³/s)	M (N•m)	w (rad/s)	P_{mec} (W)	h (m)	P_h (W)	η (%)
0.167	-164.9	-140	23086	17.63	28813	80	0.218	-220.6	-140	30884	21.00	44859	69
0.150	-136.3	-140	19082	14.31	21034	91	0.156	-112.4	-140	15742	10.80	16512	95
0.183	-204.2	-140	28588	21.27	38149	75	0.171	-136.1	-140	19054	13.03	21844	87
0.140	-118.5	-140	16590	12.49	17139	97	0.187	-162.0	-140	22680	15.47	28359	80
0.145	-127.3	-140	17815	13.39	19022	94	0.202	-190.2	-140	26628	18.13	35884	74
0.117	-82.2	-120	9869	8.71	9966	99	0.140	-91.1	-120	10932	8.75	11998	91
0.133	-107.7	-120	12920	11.33	14816	87	0.149	-103.7	-120	12444	9.94	14513	86
0.123	-92.0	-120	11039	9.72	11752	94	0.156	-112.5	-120	13500	10.77	16439	82
0.127	-97.1	-120	11647	10.24	12744	91	0.171	-136.2	-120	16344	13.00	21791	75
0.150	-136.5	-120	16384	14.29	21011	78	0.187	-162.0	-120	19440	15.54	28477	68
0.117	-82.5	-100	8245	8.69	9947	83	0.202	-190.3	-120	22830	18.10	35821	64
0.133	-107.9	-100	10792	11.31	14741	73	0.109	-55.1	-100	5510	5.31	5673	97

To be continued

Continued

5 blades (200mm)							4 blades (200 mm)					
Q_{ef}(m³/s)	M (N•m)	w (rad/s)	P_{mec}(W)	h (m)	P_h(W)	η (%)	Q_{ef}(m³/s)	M (N•m)	w (rad/s)	P_{mec}(W)	h (m)	P_h(W)	η (%)
0.100	-60.4	-100	6039	6.42	6290	96	0.125	-72.0	-100	7198	6.91	8462	85
0.107	-68.8	-100	6880	7.29	7623	90	0.140	-91.1	-100	9115	8.72	11964	76
0.084	-40.0	-90	3600	4.48	3688	98	0.156	-112.6	-100	11256	10.74	16422	69
0.100	-60.5	-90	5445	6.41	6284	87	0.109	-55.1	-90	4960	5.30	5658	88
0.117	-85.6	-90	7704	8.68	9957	77	0.125	-72.0	-90	6480	6.90	8450	77
0.093	-52.6	-90	4736	5.60	5102	93	0.140	-91.2	-90	8208	8.71	11955	69
0.150	-136.9	-90	12321	14.26	20968	59	0.156	-112.6	-90	10134	10.73	16411	62

Table 3 presents some reference values obtained by CFD modeling for an impeller diameter of 200 mm, with 4 and 5 blades. These values represent a wide range of operation for different rotational speed, discharge and head values.

Based on CFD 3D hydrodynamic simulations for small discharge range values, performance curves are obtained based on the following dimensionless parameters:

$$\text{Discharge number: } \varphi = \frac{Q}{ND^3} \qquad (26)$$

$$\text{Head number: } \psi = \frac{gH}{N^2D^2} \qquad (27)$$

$$\text{Power number: } \Pi = \frac{P_{mec}}{\rho\, N^3 D^5} \qquad (28)$$

Figure 8 shows the performance curves for head and power number and efficiency versus discharge number variation for the tubular propeller of D =100 mm with four and five blades, respectively.
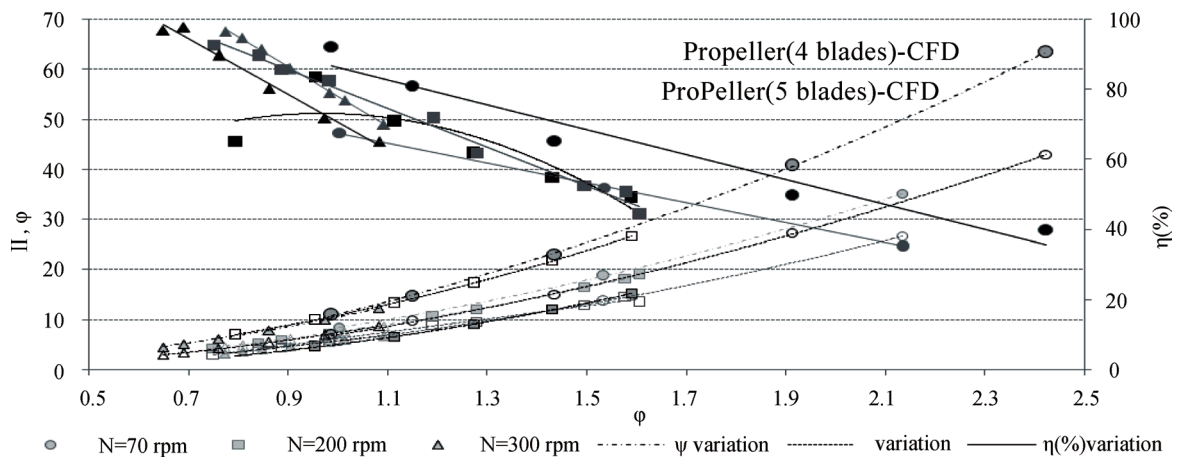

Figure 8
Comparison of Power and Head Numbers and Efficiency vs Discharge Number for 4 and 5 Blades Propellers of D = 100mm

For the impeller with 4 blades the BEP is obtained for a rotational speed of 300 rpm (N_{sqt} = 91 rpm (m, m³/s)), a discharge of 4 l/s. The BEP for the propeller with five blades is obtained for a discharge of 3.4 l/s, a rotational speed of 300 rpm (N_{sqt} = 80 rpm (m, m³/s)).

3.2 Hydrodynamic Behaviour
Established the BEP for the tubular propellers (with four and five blades) based on CFD simulations, detailed analyses are developed in order to better understand the 3D hydrodynamic behaviour of the flow throughout each impeller. For the tubular propeller (D = 100 mm) with five blades and according to a discharge, rotational speed and head, the flow velocities, total pressure, turbulence intensity, wall shear stress and pathlines are presented in Figure 9.
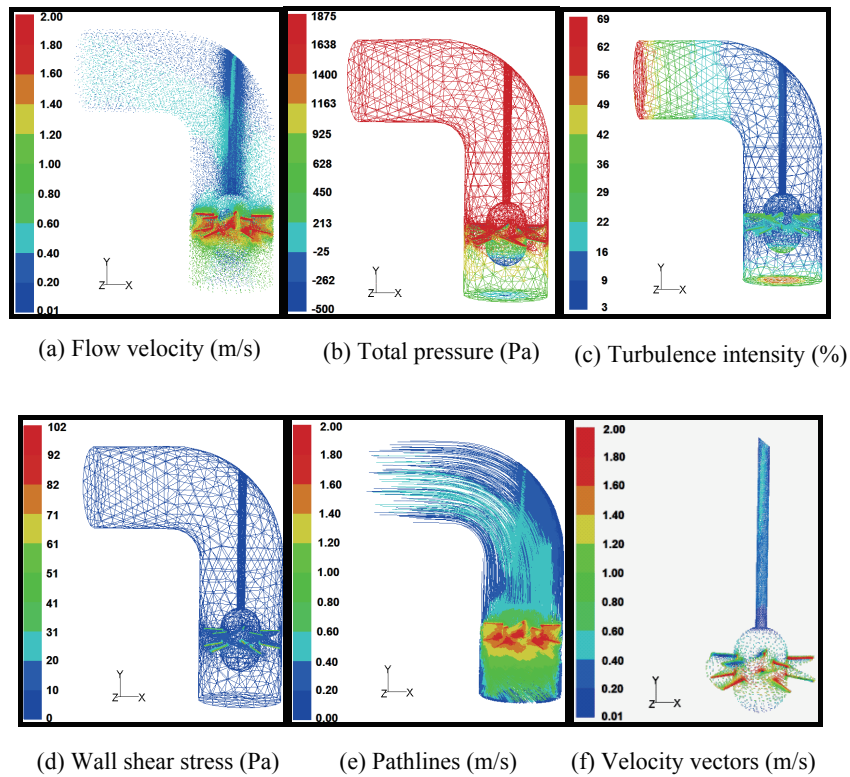
(a) Flow velocity (m/s)   (b) Total pressure (Pa)   (c) Turbulence intensity (%)

(d) Wall shear stress (Pa)   (e) Pathlines (m/s)   (f) Velocity vectors (m/s)

Figure 9
Fluid Performance Inside Tubular Propeller with Five Blades

(a) Flow velocity (m/s)   (b) Total pressure (Pa)   (c) Turbulence intensity (%)

(d) Wall shear stress (Pa)   (e) Pathlines (m/s)   (f) Velocity vectors (m/s)
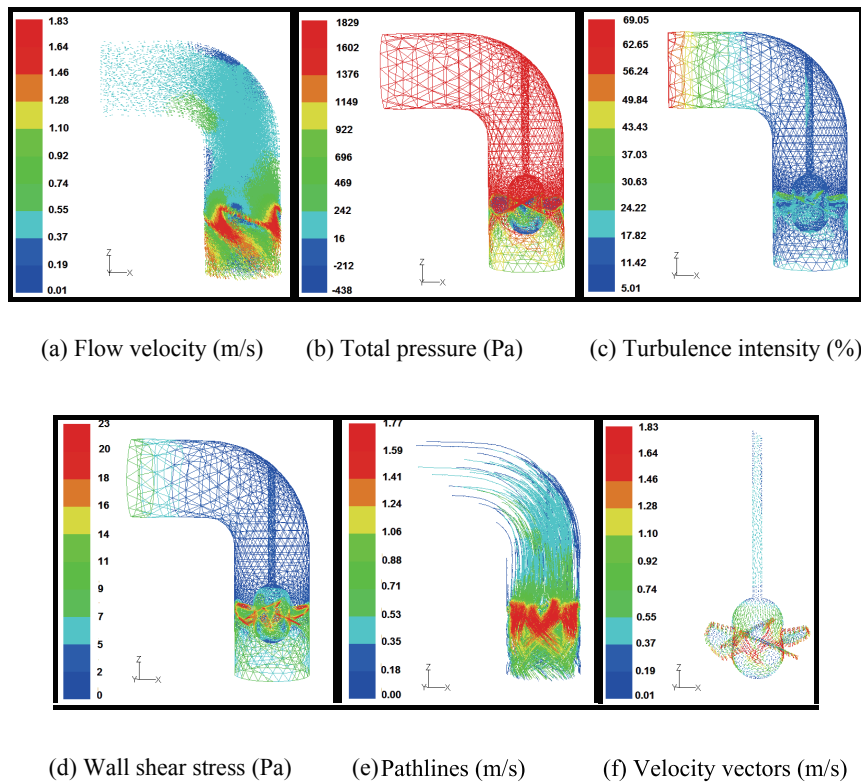
Figure 10
Fluid Performance Inside Tubular Propeller with Four Blades

This 3D fluid computational analysis considers steady pressurized flow conditions, keeping a constant rotational speed where the singularities reflect an increasing of turbulence. Analysing Figure 9, there are some instabilities in the flow inside the turbine. This is not only due to the rotation of the impeller as it is associated to the circulation flow, making an anisotropic behaviour in different turbine zones, but also the way of the flow enters into the turbine section, through the propeller and leaves with a rotational movement (in vortex configuration) towards the draft tube or downstream pipe.

Given the characteristic curves of the tubular propeller with four blades, and after established the BEP, it is observed a similar behaviour for the velocity, pressure, turbulence, shear stress, and pathlines as showed in Figure 10.

At upstream of the turbine, the flow has a low velocity, with higher pressure values in this region, presenting irrotacional behaviour. However, when it enters in the field of the impeller rotation, the flow becomes a rotational behaviour. At turbine section, the flow goes through the impeller being influenced by the impeller contour inducing the effect of flow separation with significant effects on the turbulence intensity and wall shear stress. It is also noticed the shear stress is higher near the periphery of the blades conferring some significant flow resistance in this zone.

For these tubular turbines are specified four sectioning plans (Figure 11) to analyse the behaviour of the flow in zones where the flow range can vary and where it is needed a better comprehension about the variation of the flow velocity.
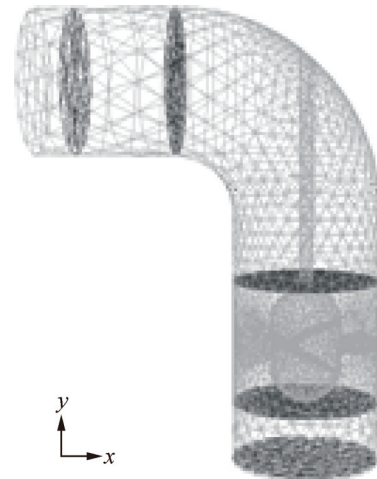

Figure 11
Schematic Representations of the Sectioning Plans for Instantaneous Velocity Analysis

In Figure 12 the fluid enters the turbine with an average speed of 0.32 m/s, decreasing as it approaches the tubular walls due to the well known effect of wall friction effect. As it approaches the curve and the impeller, the flow presents asymmetry behaviour in the velocity distribution.

In Figure 13 the velocity distribution shows a similar behaviour. Along the axis the flow tends to be influenced by the shaft rotation inducing the formation of separation zones.
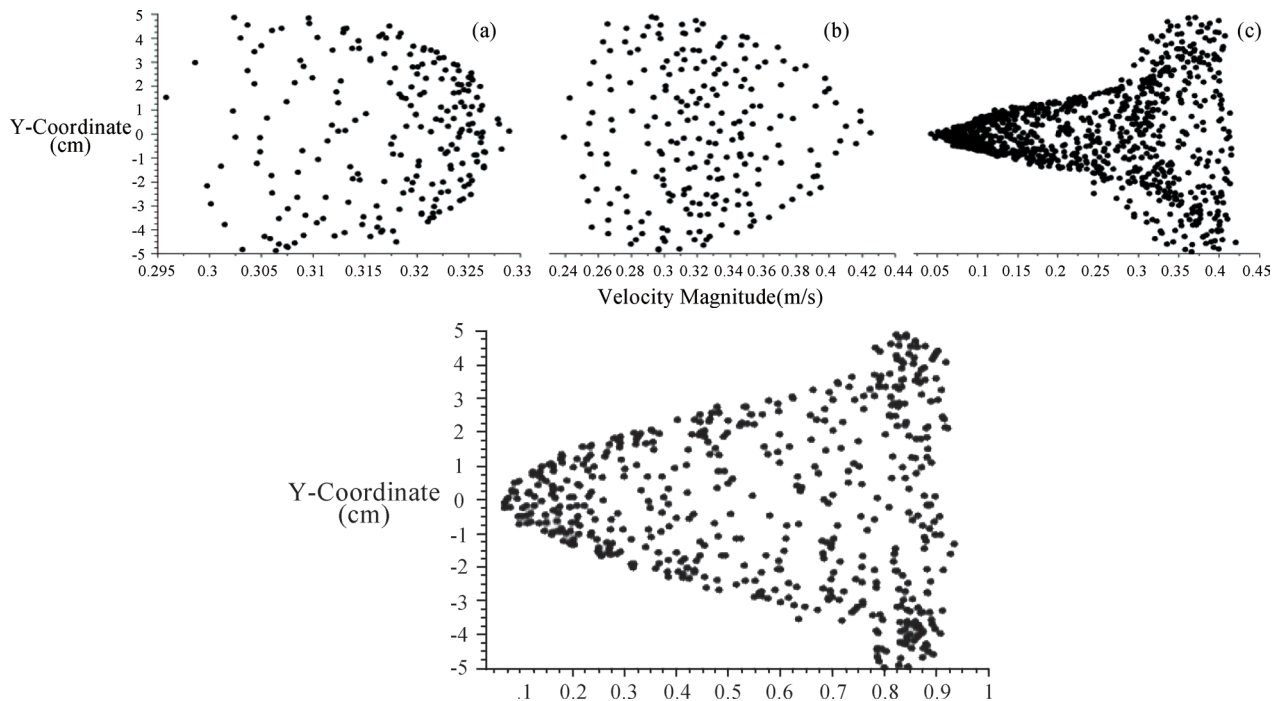

Figure 12
CFD Simulations for the Variation of the Flow Velocity Across Turbine with Five Blades
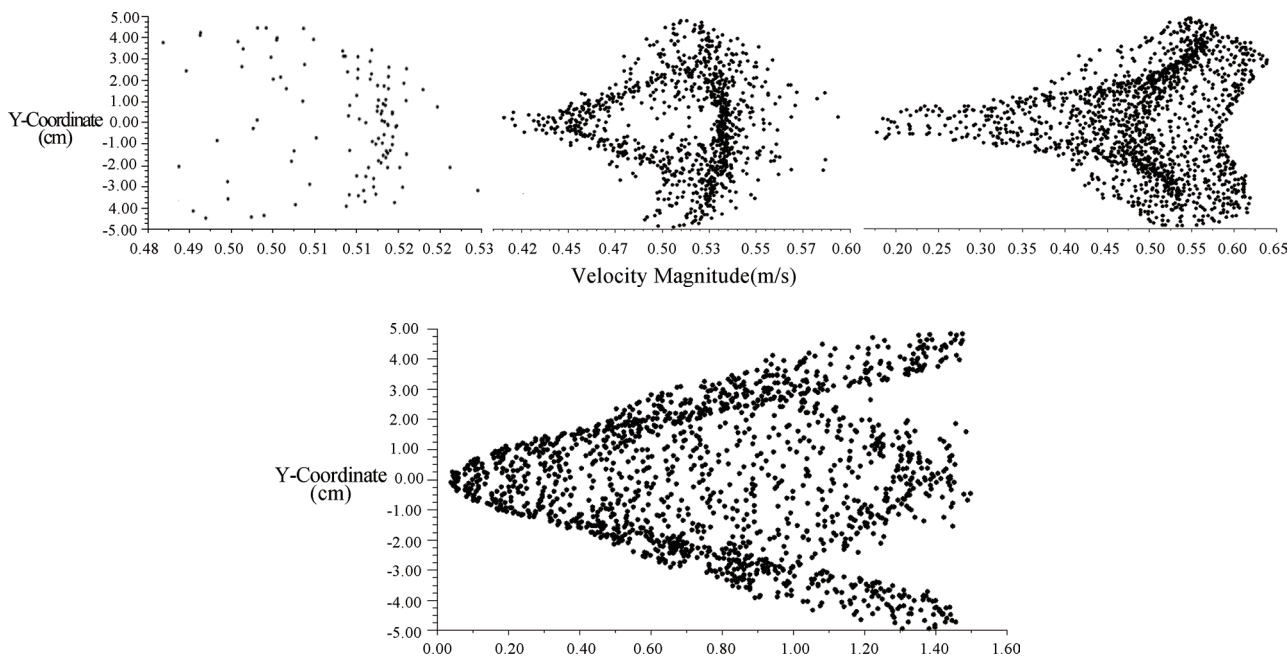
Figure 13
CFD Simulations for the Variation of the Flow Velocity Across Turbine with Four Blades

Although the number of blades are different, in general way the hydrodynamic behaviour is similar. Comparing Figure 12 and Figure 13, there is an agreement associated with the effects of the flow rotation, the friction and the existence of seperation zones, which induce a variation behaviour along the turbine, which is the base of the efficiency variation for different operational conditions.

4. EXPERIMENTAL TESTS

Figure 14 shows the schematic facility for the analysis of the propeller turbines with five and four blades and an impeller diameter of D =100 mm placed in a loop pipe in order to maintain a steady state flow conditions. This setup comprises a pipe system with a pump, for the recirculation, an air vessel to control the pressure at upstream, an electromagnetic flow meter and a downstream reservoir provided with a triangular (90º) weir. There is a valve for the flow control at downstream the air vessel and when it is fully open the maximum possible turbine flow is 5.2 l/s.

Through the turbine upstream curve, the shaft transmits the momentum to a torque balance or a generator.

During the tests it was observed an isotropic behaviour of the flow at upstream of the turbine and an anisotropy through the impeller influenced by the flow rotation and separation of the boundary layer that exists at downstream of the internal impeller bulb. The BEP for the tubular propeller (D =100 mm) under lab conditions is for a rotation speed of 200 rpm (N_{sqt} = 84 rpm (m, m^3/s)), as shown in Figure 15, with dimensionless curves based on head number and efficiency versus discharge number for the impeller with four and five blades, respectively.
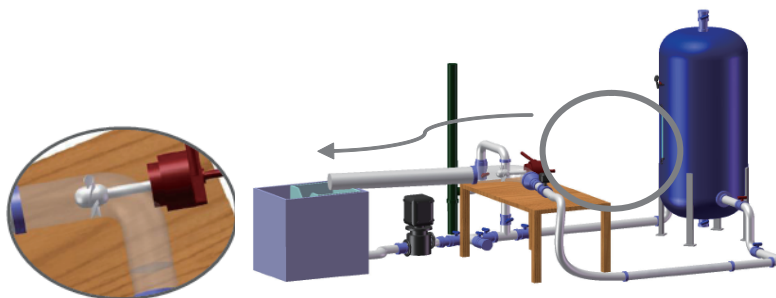

Figure 14
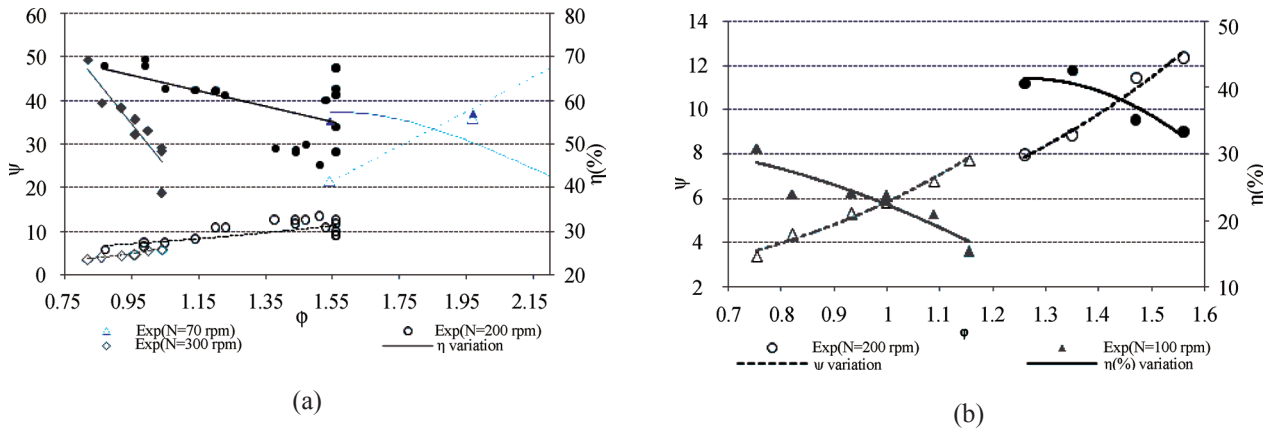**Tubular Propeller Installation**

(a)

(b)

Figure 15
Characteristics Curves of Tubular Propeller: (a) with Four Blades; (b) with Five Blades

The behaviour of tubular turbine with five blades (Figure 15 (b)) shows that this turbine is most adequate to operate with higher discharge values that there are not available in the facility.

According to the lab conditions, the experiments are obtained by regulating the discharge control valve, measuring the runner speed in a tachometer Hibok-24 for different flow values measured in an electromagnetic flow meter, and pressure head in transducers at upstream and downstream of the turbine, in undisturbed flow zones. These measurements are then compared with the CFD-3D model simulations. Using an Ultrasonic Doppler Velocimetry (UDV) in the zone of the turbine (Figure 16), the velocity profiles throughout the system are analyzed. With the UDV sample placed on vertical-sloped position of 25º, this device measures the flow velocities allowing the evaluation of the flow behaviour in real time.
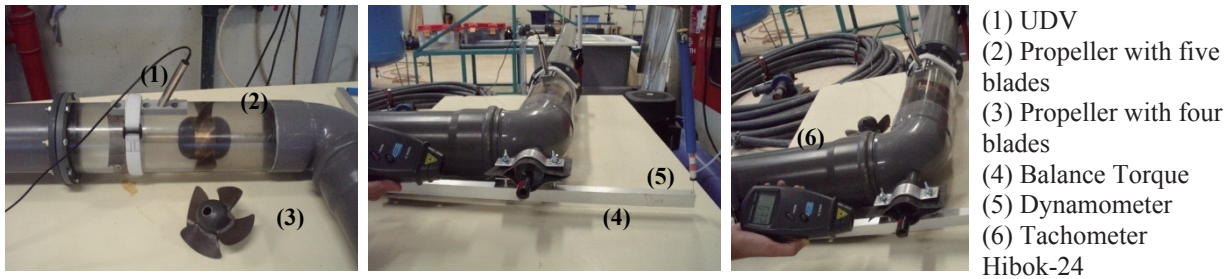

(1) UDV
(2) Propeller with five blades
(3) Propeller with four blades
(4) Balance Torque
(5) Dynamometer
(6) Tachometer Hibok-24

Figure 16
Experimental Facility of the Tubular Propeller: UDV (Left); Balance Torque (Center); Rotational Speed Measurement (Right)
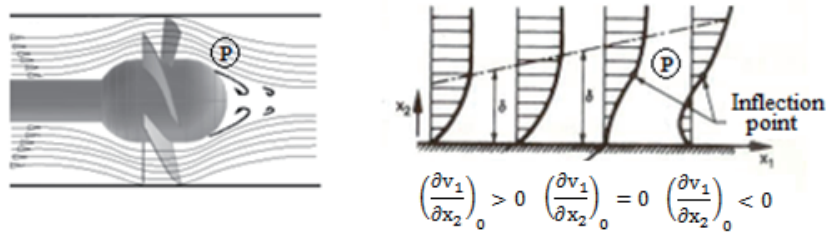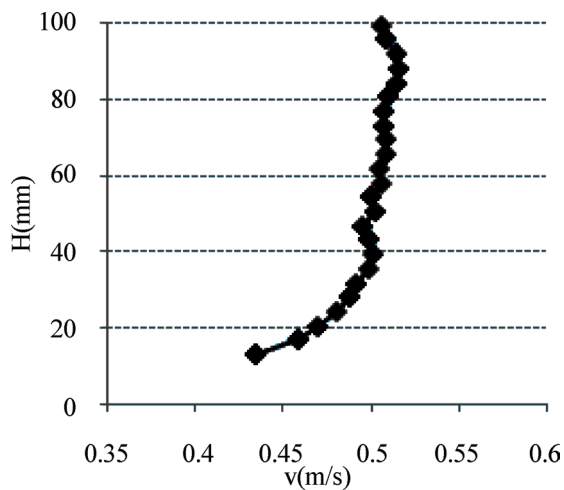

Figure 17
Separation of the Boundary Layer and Velocity Profiles

Figure 17 shows different velocity profiles along a runner boundary layer, where they represent the behaviour of the flow separation zone in which the velocity profile inversion tendency is visible.

The most important features to retain in the identification of a turbulent flow are essentially through (i) the flow irregularity by the occurrence of three-dimensional vorticity fluctuations, i.e. the turbulent movements are rotational, (ii) the continuity valid for the turbulent movements, since the smallest scales of these vortices are generally superior to the molecular fluid scale, (iii) the energy dissipation, i.e. the turbulent phenomenon is associated to a significant energy loss, where the turbulence is damped quickly by giving a greater homogeneity and isotropy to the flow motion, (iv) the diffusivity corresponding to a rapid mixing within the

fluid domain, followed by transfer of momentum, heat and mass in rapid variations or fluctuations in the flow.
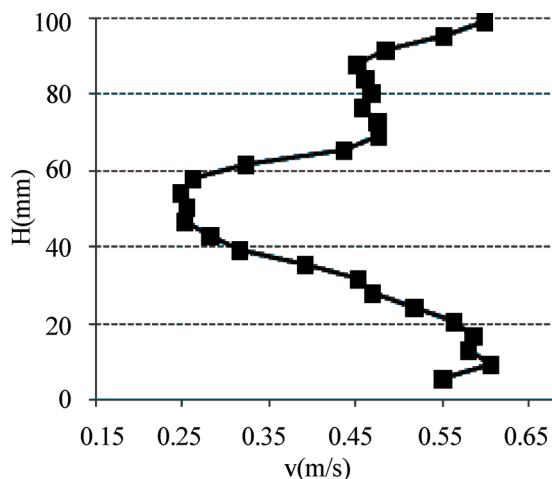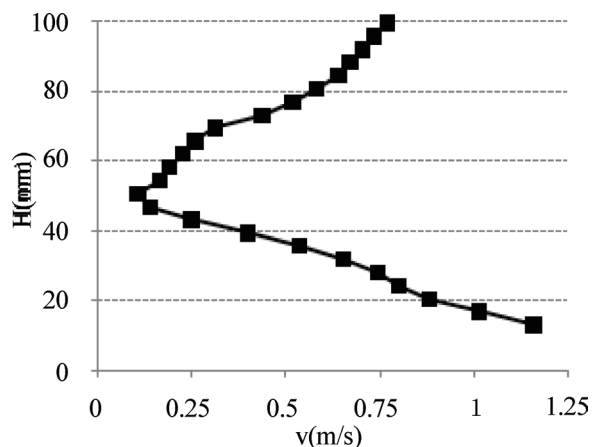
Based on these premises, Figure 18 shows the mean velocity profiles along the turbine for the plans referenced in Figure 11.

(a)
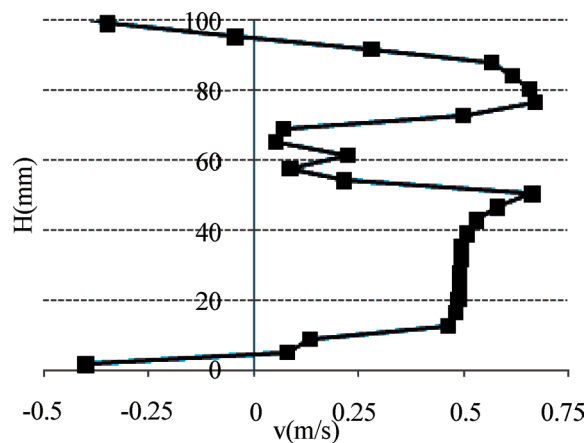
(b)

(c)

(d)

Figure 18
Flow Velocity Profiles Obtained by UDV in Sections Represented in Figure 12 (a) to (d)

From these profiles and comparing Figure 18 with Figure 13 a similar behaviour of the fluid is visible, as well as the identification of the section where the separation effect is notorious. When the fluid comes closer to the curve there is certain anisotropy with velocity retardation induced by the shaft rotation, and as soon it passes through the bulb the pressure and velocity decreases induced by the depression existed at downstream the impeller, leading to a separate zone (Ramos *et al.*, 2012). When a fluid moves in the turbulent regime, its domain can be subdivided into two regions, where the movement has its own characteristics: a thin layer near the solid walls in which the tangential stress play an important role (the boundary layer); and the remaining part occupied by the fluid field, where the shear stress is presented with less significance.

5. COMPARISON OF PERFORMANCE CURVES

Dimensionless characteristic parameters of CFD simulations and lab tests were selected and compared as shown in Figure 19, in which H_0 and Q_0 are the rated values of head and discharge. The comparison of CFD simulations for the two impellers (i.e. with five and four blades) with the lab tests shows typical trends and a reasonable fit in the head performance behaviour.
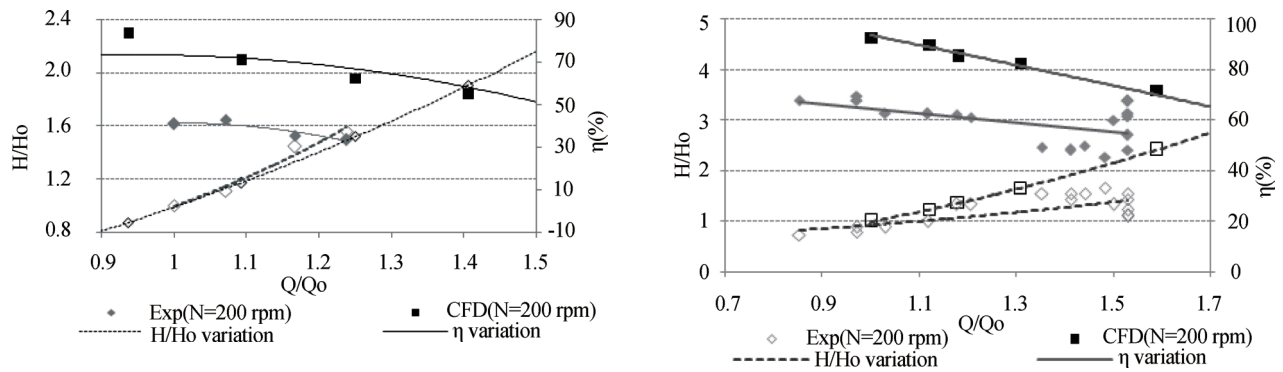
Figure 19
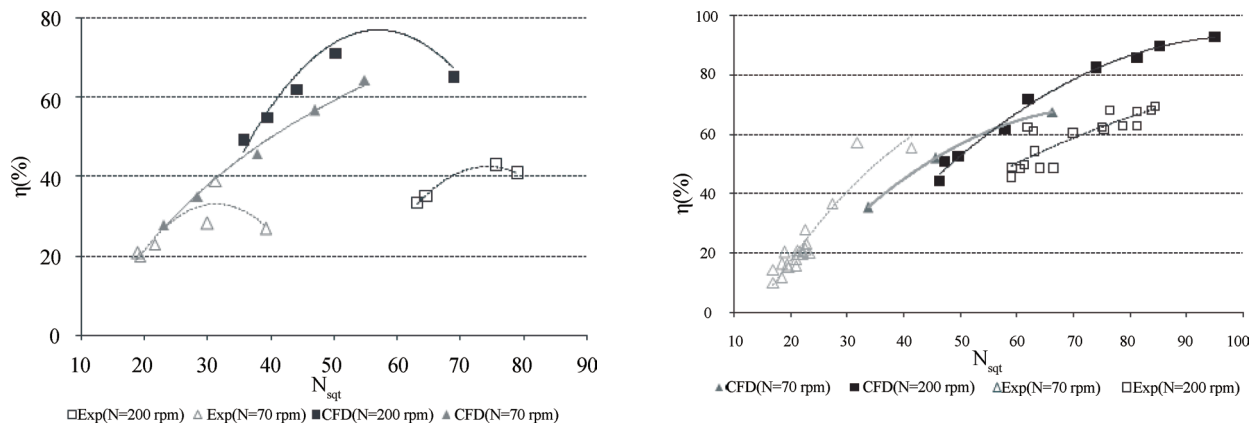**Comparison Between CFD Simulations and Experimental Results of Tubular Propellers**

Figure 20
Performance Curves Between CFD Simulations and Experimental Results: (a) Turbine Tubular Propeller with Five Blades; (b) Turbine Tubular Propeller with Four Blades

Regarding the efficiency values it is noticed a discrepancy justified by scale and losses effects that the CFD does not take into account in the simulations. Figure 20 presents comparisons between efficiency vs specific speed (m, m³/s) curves two rotational speed values (i.e. 70 and 200 rpm). The efficiency values by CFD analyses are higher than the experimental ones, essentially due to negligible factor owing to the friction losses in the mechanical system, such as bearings and seals that CFD codes cannot perform.

In Figure 20 (a), as increasing the rotational speed, there is a higher difference between simulations and tests, due to lab discharge limitations, forcing the propeller with five blades to run out of the optimal operation point. For the propeller with four blades, Figure 20 (b), the lab conditions are much closer to the rated operating point and consequently the results fit better.

CONCLUSIONS

Optimizing analyses for new tubular propellers (with five and four blades) adequate for low-head pipe systems and small discharge values are key solutions of the utmost interest to water companies to supply energy to data acquisition systems, control of the operational management in rural and isolated areas or even supply renewable energy to small regions, where it is very expensive to extend the energy line to these locations. These solutions are also adequate for small pumping systems and water treatment plants. The proposed new tubular propeller turbines (with 4 and 5 blades) represent a cheap, easy installation, good performances and competitive solutions to cover a power, head and discharge values lower than 8 kW, 20 m and 200 l/s respectively, corresponding a range of application not obtainable for existent commercial turbines available in the market.

These devices can be installed at the entrance and the exit of reservoirs or tanks or in some off-grid treatment plants, where are located the most electromechanical equipment which needs energy, or even in pipe systems for water drinking or drainage, where is necessary to provide power to supply control systems or for collect data.

Table 4
Main Characteristics of New Tubular Propeller for Low-Head Solutions

Turbine	D	H₀	Q₀	N₀	η_max	P_mec	Range of application		
	(mm)	(m)	(m³/s)	(r/m)	(%)	(W)	Q (10^{-3}m³/s)	H (m)	N (r/m)
Propeller with 5 blades	100[1]	0.13	0.0034	300	98	4	2.5-5	0.08-0.3	200-300
	100[2]	0.13	0.0049	200	35	2	2.5-5	0.04-0.17	70-200
	200[3]	8.77	0.092	1146	97	7660	70-150	5-20	900-1400
Propeller with 4 blades	100[1]	0.12	0.004	300	95	4	3-5	0.05-0.25	200-300
	100[2]	0.07	0.0033	200	70	2	2.3-5.2	0.07-0.15	70-300
	200[3]	5.32	0.109	1000	97	5510	110-200	5-18	900-1400

[1] CFD analysis for lab conditions; [2] Experimental tests; [3] CFD turbomachine similarity from a propeller with 100 mm

Table 4 shows a summary of the main characteristics of the converters developed in this study which aim at providing small power outputs, usually available in most of the pressurized pipe systems.

A significant range of possible applications is presented in which traditional turbines cannot still cover in a cost-effective manner. These machines are economic solutions, because they are quite simple, normally composed by a runner installed in a pipe-curve, without volute, neither a guide vane. They are appropriate for operation under almost constant-flow conditions, as for water pipe systems equipped with a discharge control valve.

Fluid computational 3D analysis together with a blade model configuration (BMC) and experimental tests help to better understand the phenomenon associated with the hydrodynamic and turbine behaviour, leading a greater knowledge of interaction between the machine geometry, the hydraulic flow conditions and the turbine performance. These developments allow finding the best solution in terms of design, behaviour and configuration, whereby a good basis of calculations has become a point of promising research. This work provides also a good guideline for possible new design of low power turbines in order to highlight the continuity development of new energy converters to support cost-effective micro-hydro solutions.

ACKNOWLEDGMENTS

REFERENCES

[1] Howey, D. A. (2009). Axial Flux Permanent Magnet Generators for Pico-Hydropower. EWB-UK Research Conference 2009, Hosted by the Royal Academy of Engineering, February 20th.

[2] Simpson, R. G., & Williams, A. A. (2006). Application of Computational Fluid Dynamics to the Design of Pico Propeller Turbines. ICREDC-06, School of Engineering and Applied Sciences, University of the District of Columbia, Washington DC, USA.

[3] Demetriades, G. M. (1997). *Design of Low-Cost Propeller Turbines for Standalone Micro-hydroelectric Generation Units* (Doctoral Dissertation). University of Nottingham, UK.

[4] Upadhyay, D. (2004). *Low Head Turbine Development Using Computational Fluid Dynamics* (Doctoral Dissertation). University of Nottingham, UK.

[5] Alexander, K. V., Giddens, E. P., & Fuller, A. M. (2009). Axial-Flow Turbines for Microhydro Systems. *Elsevier Journal of Renewable Energy*, *34*, 35-47.

[6] Skotak, A., Mikulasek, J., & Obrovsky, J. (2009). Development of the New High Specific Speed Fixed Blade Turbine Runner. *International Journal of Fluid Machinery and Systems*, *2*(4).

[7] Ramos, H. M., Borga, A., & Simão, M. (2009). New Design Solutions for Low-Power Energy Production in Water Pipe Systems. *Water Science and Engineering*, *2*(4), 69-84. doi:10.3882/j.issn.1674-2370.2009.04.007

[8] Ramos, H. M., Borga, A., & Simão, M. (2010). *Energy Production in Water Supply Systems: Computational Analysis for New Design Solutions*. London, Taylor & Francis Group.

[9] Fluent 6.3. (2006). *User's Guide*. USA.

[10] Scott-Pomerantz, C. D. (2004). *The k-Epsilon Model in the Theory of Turbulence* (Doctoral Dissertation). University of Pittsburg, USA.

[11] Ansys CFX 11.0. (2006). *Tutorials*. PA 15317, South Pointe 275 Technology Drive, Canonsburg.

[12] Ramos, H. M., Borga, A., & Simão, M. (2009). Cost-Effective Energy Production in Water Pipe Systems: Theoretical Analysis for New Design Solutions. 33rd IAHR Congress. *Water Engineering for a Sustainable Environment*. Managed by EWRI of ASCE on behalf of IAHR. Vancouver, British Columbia, Canada, August 9-14.

[13] Ramos, H.M., Simão, M, & Kenov, K. N. (2012). Low-Head Energy Conversion: A Conceptual Design and Laboratory Investigation of a Microtubular Hydro Propeller. *International Scholarly Research Network, ISRN Mechanical Engineering, Article ID 846206*, 1-10. doi:10.5402/2012/846206